

Article

Asymmetries in Processes of Electron–Positron Annihilation

Andrej Arbuzov ^{1,2,*}, Serge Bondarenko ^{1,†} and Lidia Kalinovskaya ^{3,†}¹ Bogoliubov Laboratory of Theoretical Physics, JINR, Joliot-Curie str. 6, 141980 Dubna, Russia; bondarenko@jinr.ru² Dubna State University, Universitetskaya str. 19, 141982 Dubna, Russia³ Dzhelapov Laboratory of Nuclear Problems, JINR, Joliot-Curie str. 6, 141980 Dubna, Russia; lidia.kalinovskaya@cern.ch

* Correspondence: arbuzov@theor.jinr.ru

† These authors contributed equally to this work.

Received: 14 June 2020; Accepted: 6 July 2020; Published: 7 July 2020



Abstract: Processes of electron–positron annihilation into a pair of fermions were considered. Forward–backward and left–right asymmetries were studied, taking into account polarization of initial and final particles. Complete 1-loop electroweak radiative corrections were included. A wide energy range including the Z boson peak and higher energies relevant for future e^+e^- colliders was covered. Sensitivity of observable asymmetries to the electroweak mixing angle and fermion weak coupling was discussed.

Keywords: high energy physics; electron–positron annihilation; forward–backward asymmetry; left–right asymmetry

PACS: 12.15.-y; 12.15.Lk; 13.66.Jn

1. Introduction

Symmetries play a key role in the construction of physical theories. In fact, they allow us to describe a huge variety of observables by means of compact formulae. We believe that the success of theoretical models based on symmetry principles is due to the presence of the corresponding properties in Nature. The Standard Model (SM) is the most successful physical theory ever. Its predictions are in excellent agreement with practically all experimental results in particle physics. The renormalizability of the model allows us to preserve unitarity and provide finite verifiable results. Both phenomenological achievements and nice theoretical features of the SM are mainly due to the extended usage of symmetries in its construction. The model is based on several symmetries of different type, including the Lorentz (Poincaré) symmetry, the gauge $SU(3)_C \times SU(2)_L \times U(1)_Y$ symmetries, the CPT symmetry, the spontaneously broken global $SU(2)_L \times SU(2)_R$ symmetry in the Higgs sector, etc. Some symmetries of the model are exact (or seem to be exact within the present precision) while others are spontaneously or explicitly broken. In particular, the nature of the symmetry among the three generations of fermions is one of the most serious puzzles in the SM and verification of the lepton universality hypothesis is on the task list of modern experiments.

Despite the great successes of the SM, we can hardly believe that it is the true fundamental theory of Nature. Most likely, it is an effective model with a limited applicability domain. The search for the upper energy limit of the SM applicability is the actual task at all high-energy colliders experiments. Up to now, all direct attempts to find elementary particles and interactions beyond the Standard Model have failed. The accent of experimental studies has shifted towards accurate verification of the SM features. Deep investigation of the SM symmetries is an important tool in this line of research.

Asymmetries form a special class of experimental observables. First of all, they explicitly access the breaking of a certain symmetry in Nature. Second, they are usually constructed as a ratio of observed quantities, in which the bulk of experimental and theoretical systematic uncertainties is canceled out. So the asymmetries provide independent additional information on particle interactions. They are especially sensitive to non-standard weak interactions including contributions of right currents and new intermediate Z' vector bosons, see e.g., [1].

The physical programs of future (super) high-energy electron–positron colliders such as CLIC [2], ILC [3–5], FCC-ee [6], and CEPC [7] necessarily include accurate tests of the SM. Studies of polarization effects and asymmetries will be important to probe of the fundamental properties of Higgs boson(s) and, in particular, in the process of annihilation into top quarks [8–10]. The future colliders plan to start operation in the so-called GigaZ mode at the Z peak and improve upon the LEP both in statistical and systematical uncertainties in tests of the SM [11] by at least one order of magnitude. Among these collider projects, the FCC-ee one has the most advanced program of high-precision measurements of SM processes at the Z peak. Such tests have been performed at LEP and SLC and they have confirmed the validity of the SM at the electroweak (EW) energy scale of about 100 GeV [12,13]. During the LEP era, extensive experimental and theoretical studies of asymmetries made an important contribution to the overall verification of the SM, see review [14] and references therein. The new precision level of future experiments motivates us to revisit the asymmetries and scrutinize the effects of radiative corrections (RCs) to them. In the analysis of LEP data, semi-analytic computer codes like ZFITTER [15] and TOPAZ0 [16] were extensively used. The forthcoming new generation of experiment requires more advanced programs, primarily Monte Carlo event generators.

The article is organized as follows. The next section contains preliminary remarks and the general notations. Section 3 is devoted to the left–right asymmetry. The forward–backward asymmetry is considered in Section 4. Discussion of the left–right forward–backward asymmetry is presented in Section 5. In Section 6, we provide results related to the final state fermion polarization. Section 7 contains a discussion and conclusions.

2. Preliminaries and Notations

In the recent paper [17] by the SANC group, high-precision theoretical predictions for the process $e^+e^- \rightarrow l^+l^-$ ($l = \mu$ or τ) were presented. With the help of computer system SANC [18], we calculated the complete 1-loop electroweak radiative corrections to these processes, taking into account possible longitudinal polarization of the initial beams. The calculations were performed within the helicity amplitude formalism, taking into account the initial and final state fermion masses. So, the SANC system provides a solid framework to access asymmetries in e^+e^- annihilation processes and to study various relevant effects. In particular, the system allows us to separate effects due to quantum electrodynamics (QED) and weak radiative corrections.

The focus of this article is on the description and assessment of the asymmetry family: the left–right asymmetry A_{LR} , the forward–backward asymmetry A_{FB} , the left–right forward–backward asymmetry A_{LRFB} , and the final state fermion polarization P_f in collisions of high-energy polarized or unpolarized e^+e^- beams. The main aim was to verify the effect of radiative corrections on the extraction of the SM parameters from the asymmetries and to analyze the corresponding theoretical uncertainty.

We performed calculations for polarized initial and final state particles. Beam polarizations play an important role:

- They improve the sensitivity to CP-violating anomalous couplings or form factors, which are measurable even with unpolarized beams through the forward–backward asymmetry.
- With the polarization of both beams, the sensitivity to the new physics scale can be increased by a factor of up to 1.3 with respect to the case with only polarized electrons [1].
- A high-luminosity at the GigaZ stage of a collider running at the Z boson resonance with positron polarization allows us to improve the accuracy of the determination of $\sin^2 \theta_W$ (θ_W is

the electroweak mixing angle) by an order of magnitude, through studies of the left–right asymmetry [1].

Numerical illustrations for each asymmetry are given in two energy domains: the wide center-of-mass energy range $20 \leq \sqrt{s} \leq 500$ GeV and the narrow one around the Z resonance ($70 \leq \sqrt{s} \leq 100$ GeV), where a peculiar behavior of observables can be seen. All results were produced with the help of the e^+e^- branch [19] of the MCSANC Monte Carlo integrator [20].

Let us introduce the notation. First of all, we define quantities A_f ($f = e, \mu, \tau$) which are often used for description of asymmetries at the Z peak:

$$A_f \equiv 2 \frac{g_{V_f} g_{A_f}}{g_{V_f}^2 + g_{A_f}^2} = \frac{1 - (g_{R_f}/g_{L_f})^2}{1 + (g_{R_f}^2/g_{L_f}^2)^2}, \quad (1)$$

where the vector and axial-vector coupling constants of the weak neutral current of the fermion f with the electromagnetic charge q_f (in the units of the positron charge e) are

$$g_{V_f} \equiv I_f^3 - 2q_f \sin^2 \vartheta_W, \quad g_{A_f} \equiv I_f^3. \quad (2)$$

The corresponding left and right fermion couplings are

$$g_{L_f} \equiv I_f^3 - q_f \sin^2 \vartheta_W, \quad g_{R_f} \equiv -q_f \sin^2 \vartheta_W. \quad (3)$$

The neutral current couplings g_{L_f} and g_{R_f} quantify the strength of the interaction between the Z boson and the given chiral states of the fermion.

We claim that there are sizable corrections to all observable asymmetries due to radiative corrections which affect simple Born-level analytic formulae relating the asymmetries with electroweak parameters. It is especially interesting to consider the behavior of asymmetries in different EW schemes: $\alpha(0)$, $\alpha(M_Z^2)$, and G_μ , see their definitions below. We also will compare the results in the Born and 1-loop approximation. The latter means inclusion of 1-loop radiative corrections of one of the following types: pure QED photonic RCs (marked as “QED”), weak RCs (marked as “weak”), and the complete 1-loop electroweak RCs (marked as “EW”):

$$\sigma_{\text{EW}} = \sigma_{\text{Born}} + \sigma_{\text{QED}} + \sigma_{\text{weak}}.$$

The weak part in our notation includes 1-loop self-energy corrections to photon and Z boson propagators. In our notation, higher-order effects due to interference of pure QED and weak contributions are a part of σ_{weak} .

The cross section of a generic annihilation process of longitudinally polarized e^+ and e^- with polarization degrees P_{e^+} and P_{e^-} can be expressed as follows:

$$\begin{aligned} \sigma(P_{e^-}, P_{e^+}) &= (1 + P_{e^-})(1 + P_{e^+})\sigma_{RR} + (1 - P_{e^-})(1 + P_{e^+})\sigma_{LR} \\ &+ (1 + P_{e^-})(1 - P_{e^+})\sigma_{RL} + (1 - P_{e^-})(1 - P_{e^+})\sigma_{LL}. \end{aligned} \quad (4)$$

Here $\sigma_{ab} = \sum_{ij(k)} |\mathcal{H}_{abij(k)}|^2$ are the $2 \rightarrow 2(3)$ helicity amplitudes of the reaction, ($ab = RR, RL, LR, LL$) with right-handed $R = “+”$ or left-handed $L = “-”$ initial particles.

It is convenient to combine the electron P_{e^-} and positron P_{e^+} polarizations into the effective quantity

$$P_{\text{eff}} = \frac{P_{e^-} - P_{e^+}}{1 - P_{e^-} P_{e^+}}. \quad (5)$$

In the case when only the electron beam is polarized, the effective polarization coincides with the electron one.

To investigate theoretical uncertainties, we use the following three EW schemes:

1. the $\alpha(0)$ scheme in which the fine-structure constant $\alpha(0)$ is used as input. The contribution of RCs in this scheme is enhanced by the large logarithms of light fermion masses via $\alpha(0) \ln(s/m_f^2)$ terms.
2. The $\alpha(M_Z^2)$ scheme in which the effective electromagnetic constant $\alpha(M_Z^2)$ is used at Born level while virtual 1-loop and real photon bremsstrahlung contributions are proportional to $\alpha^2(M_Z^2)\alpha(0)$. In this scheme the virtual RCs receive contributions from the quantity $\Delta\alpha(M_Z^2)$ which describes the evolution of the electromagnetic coupling from the scale $Q^2 = 0$ to the $Q^2 = M_Z^2$ one and cancels the large terms with logarithms of light fermion masses.
3. the G_μ scheme in which the Fermi coupling constant G_μ , extracted from the muon life time, is used at the Born level while the virtual 1-loop and real photon bremsstrahlung contributions are proportional to $G_\mu^2\alpha(0)$. The virtual RCs receive contributions from the quantity Δr . Since the expression for Δr contains the $\Delta\alpha(M_Z^2)$, the large terms with logarithms of the light masses are also canceled. The quantity Δr rules the G_μ and $\alpha(0)$ relation in this scheme.

Results of fixed-order perturbative calculations in these schemes differ due to missing higher-order effects. In what follows, numerical calculations are performed in the $\alpha(0)$ EW scheme if another choice is not explicitly indicated.

3. Left–Right Asymmetry A_{LR}

A scheme to measure the A_{LR} polarization asymmetry at the Z peak was suggested in [21]. It was shown that this observable can be used as for extraction of electroweak couplings as well as for a polarimeter calibration.

If we neglect the initial electron masses, the polarized cross-section can be rewritten in the following form:

$$\sigma(P_{e^-}, P_{e^+}) = (1 - P_{e^-}P_{e^+})[1 - P_{\text{eff}}A_{LR}]\sigma_0, \quad (6)$$

where σ_0 is the unpolarized cross-section.

The left–right asymmetry in the presence of partially polarized ($|P_{\text{eff}}| < 1$) initial beams is defined as

$$A_{LR} = \frac{1}{P_{\text{eff}}} \frac{\sigma(-P_{\text{eff}}) - \sigma(P_{\text{eff}})}{\sigma(-P_{\text{eff}}) + \sigma(P_{\text{eff}})}, \quad (7)$$

where σ is the cross-section with polarization P_{eff} .

In the case of fully polarized initial particles ($|P_{e^\pm}| = 1$) the definition (7) becomes:

$$A_{LR} = \frac{\sigma_{L_e} - \sigma_{R_e}}{\sigma_{L_e} + \sigma_{R_e}}, \quad (8)$$

where L_e and R_e refer to the left and right helicity states of the incoming electron.

Equations (6) and (7) show that A_{LR} does not depend on the degree of the initial beam polarization.

This type of asymmetry is sensitive to weak interaction effects in the initial vertex. In the Born approximation at energies close to the Z resonance, it is directly related to the electron coupling:

$$A_{LR} \approx A_e. \quad (9)$$

The left–right asymmetry A_{LR} as a function of the center-of-mass system (c.m.s.) energy in the ranges $20 \leq \sqrt{s} \leq 500$ GeV (Left) and $70 \leq \sqrt{s} \leq 110$ GeV (Right) is shown in Figure 1. We explore A_{LR} in different approximations and the corresponding shifts ΔA_{LR} between the Born level and 1-loop corrected approximations taking into account either pure QED, or weak, or complete EW effects: $\Delta A_{LR} = A_{LR}(1\text{-loop corrected}) - A_{LR}(\text{Born})$. The right figure shows the behavior of A_{LR} near the Z resonance, and the value A_e at $\sqrt{s} = M_Z$ is indicated by a black dot (see (9)).

One can notice that although the total 1-loop EW corrections to the process cross-section are equal to the sum of the pure QED and weak ones, the corresponding shifts ΔA_{LR} are not additive. That is because the asymmetry is defined as a ratio and the corrections affect both the numerator and denominator.

In Figure 2 we show A_{LR} for the Born and weak 1-loop corrected levels of accuracy in different EW schemes and the corresponding shifts $\Delta A_{LR} = A_{LR}(\text{weak, some EW scheme}) - A_{LR}(\text{Born})$. We see that the effects due to weak corrections in different EW schemes behave in a similar way. Nevertheless the scheme dependence is visible within the expected precision of future measurements. The deviations between the results in different schemes can be treated as a contribution into the theoretical uncertainty due to missing higher order corrections.

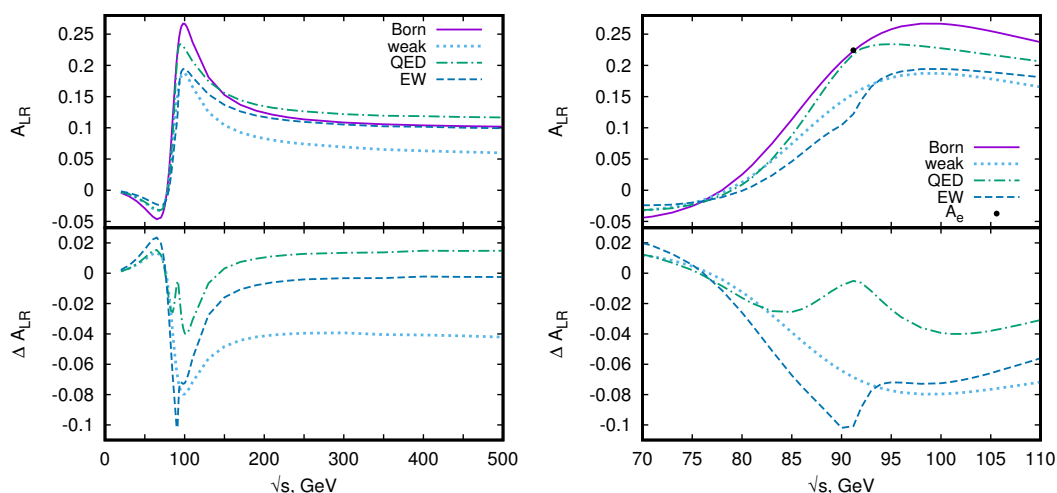


Figure 1. (Left) The A_{LR} asymmetry in the Born and 1-loop (weak, pure quantum electrodynamics (QED), and electroweak (EW)) approximations and ΔA_{LR} vs. center-of-mass system (c.m.s.) energy in a wide range; (Right) the same for the Z peak region.

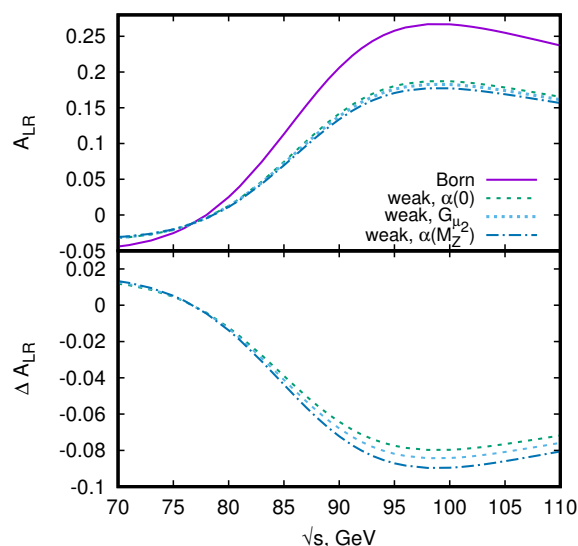


Figure 2. The A_{LR} asymmetry at the Born level and with 1-loop weak radiative corrections (RCs); the corresponding shifts ΔA_{LR} within $\alpha(0)$, G_μ , and $\alpha(M_Z^2)$ EW schemes vs. c.m.s. energy in the peak region.

The impact of 1-loop EW contributions to ΔA_{LR} is of the order -0.1 in the resonance region, but at energies above $\sqrt{s} = 200$ GeV there are considerable cancellations between weak and QED effects so that the combined EW corrections becomes small (but still numerically important for high-precision measurements).

Summary for A_{LR}

The left–right asymmetry A_{LR} is almost insensitive to the details of particle detection since the corresponding experimental uncertainties tend to cancel out in the ratio (7). It (almost) does not depend on the final state fermion couplings in the vicinity of the Z boson peak and can be measured for any final state with a large gain in statistics. For this reasons it is appropriate for extraction of the $\sin^2 \vartheta_W^{\text{eff}}$ value.

We observe that the values ΔA_{LR} due to weak and pure QED 1-loop corrections are very significant at high energies in general, but in the resonance region impact of QED is small, while the weak contribution to ΔA_{LR} reaches 0.07. Therefore, it is necessary to evaluate all possible radiative correction contributions to the weak parts of RCs carefully and thoroughly.

4. Forward–Backward Asymmetry A_{FB}

The forward–backward asymmetry is defined as

$$A_{FB} = \frac{\sigma_F - \sigma_B}{\sigma_F + \sigma_B},$$

$$\sigma_F = \int_0^1 \frac{d\sigma}{d \cos \vartheta_f} d \cos \vartheta_f, \quad \sigma_B = \int_{-1}^0 \frac{d\sigma}{d \cos \vartheta_f} d \cos \vartheta_f, \quad (10)$$

where ϑ_f is the angle between the momenta of the incoming electron and the outgoing negatively charged fermion. It can be measured in any $e^+e^- \rightarrow f\bar{f}$ channels but for precision test the most convenient channels are $f = e, \mu$. The channels with production of τ leptons, b or c quarks are very interesting as well.

At the Born level, this asymmetry is proportional to the product of initial and final state couplings and is caused by parity violation at both production and decay vertices:

$$A_{FB} \approx \frac{3}{4} A_e A_f. \quad (11)$$

In the case of partially polarized initial beams the condition (11) reduces to the following one

$$A_{FB} \approx \frac{3}{4} \frac{A_e - P_{\text{eff}}}{1 - A_e P_{\text{eff}}} A_f. \quad (12)$$

In Figure 3 we show the behavior of the A_{FB} asymmetry in the Born and 1-loop approximations (with weak, pure QED, or complete EW contributions) and the corresponding ΔA_{FB} for c.m.s. energy range $20 \leq \sqrt{s} \leq 500$ GeV in the left plot and for the Z peak region of c.m.s. energy $70 \leq \sqrt{s} \leq 110$ GeV in the right one. As in the previous case of A_{LR} , we indicate by a black dot the value $A_{FB} \approx 3/4 A_e A_\mu$ at the resonance. We observe that the weak contribution to A_{FB} is small and practically does not depend on energy. The shift ΔA_{FB} changes the sign at the resonance and tends to a constant value (~ -0.3) above 200 GeV. The huge magnitude of the shift ΔA_{FB} out of the Z resonance region is coming mainly from the pure QED corrections. In particular, above the peak the effect due to radiative return to the resonance is very important.

Figure 4 shows the dependence of A_{FB} for different levels of accuracy (Born and 1-loop weak) on the EW scheme choice: either $\alpha(0)$, or G_μ , or $\alpha(M_Z^2)$. The corresponding shifts ΔA_{FB} between the Born and the 1-loop weak corrected approximations are shown in the lower plot.

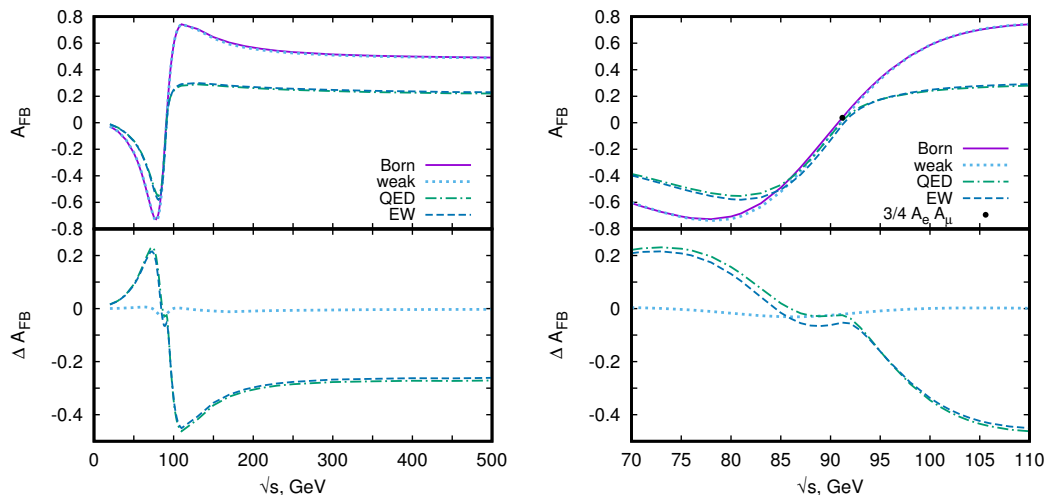


Figure 3. (Left) The A_{FB} asymmetry in the Born and 1-loop (weak, QED, EW) approximations and the corresponding shifts ΔA_{FB} for a wide c.m.s. energy range; (Right) the same for the Z peak region.

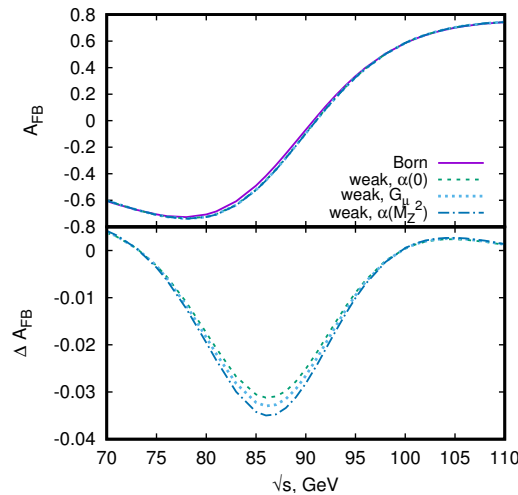


Figure 4. The A_{FB} asymmetry and ΔA_{FB} in the Born and complete 1-loop EW approximations within the $\alpha(0)$, G_μ , and $\alpha(M_Z^2)$ EW schemes vs. the c.m.s energy.

Below we investigate two sets of polarization degree $P_i = (P_{e^-}, P_{e^+})$:

$$P_1 = (-0.8, 0.3) \quad \text{and} \quad P_2 = (0.8, -0.3). \quad (13)$$

In Figure 5 we compare the values of A_{FB} asymmetry and the corresponding shifts due to EW corrections for the unpolarized case and two choices of polarized beams defined in the above equation. One can see that a combination of polarization degrees of initial particles can either increase or decrease the magnitude of the A_{FB} asymmetry with respect to the unpolarized case.

There is an interesting idea [22] to use the A_{FB} asymmetry at the FCC-ee in order to directly access the value of QED running coupling at M_Z . This idea was supported in [23] where it was demonstrated that higher-order QED radiative corrections to A_{FB} are under control. Our results show that higher-order effects due to weak interactions are not negligible in this observable; further studies are required.

At the Born level there are contributions suppressed by the small factor m_f^2/s with the fermion mass squared. It is interesting to note that in 1-loop radiative corrections there are contributions of the relative order $\alpha \cdot m_f/\sqrt{s}$ with the fermion mass to the first power [24], which are numerically relevant at high energies especially for the b quark channel.

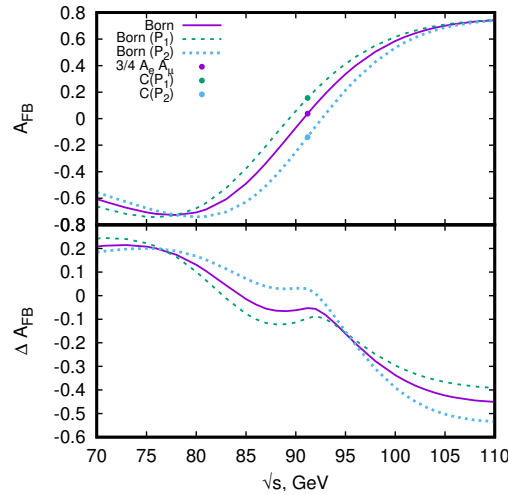


Figure 5. The A_{FB} asymmetry at the Born level (upper panel) and the corresponding ΔA_{FB} in the 1-loop EW approximation (bottom panel) for unpolarized and polarized cases with degrees of beam polarizations $P_{1,2}$ (13) vs. c.m.s. energy in the Z peak region. The constants $C(P_{1,2})$ stand for the expression (12) with polarization degrees (13).

Summary for A_{FB}

The weak 1-loop contribution ΔA_{FB} is rather small for the whole energy range, see Figure 3. Nevertheless in this asymmetry the difference between the pure QED and the complete 1-loop approximations near the resonance is numerically important. The dependence on the EW scheme choice, see Figure 4, is small but still relevant for high-precision measurements. The dependence of this asymmetry on polarization is very significant.

5. Left–Right Forward–Backward Asymmetry A_{LRFB}

In order to measure the weak couplings of the final state fermions, it was suggested to analyze the so-called left–right forward–backward asymmetry [25]:

$$A_{LRFB} = \frac{(\sigma_{Le} - \sigma_{Re})_F - (\sigma_{Le} - \sigma_{Re})_B}{(\sigma_{Le} + \sigma_{Re})_F + (\sigma_{Le} + \sigma_{Re})_B}, \quad (14)$$

where σ_L and σ_R are the cross sections with left and right handed helicities of the initial electrons.

From the definition (14) it follows that A_{LRFB} partially inherits the properties of the A_{LR} and, in particular, does not depend on the degree of the initial beam polarizations.

In the case of unpolarized beams on the Z resonance peak, the Born-level asymmetry is

$$A_{LRFB} \approx \frac{3}{4} A_f. \quad (15)$$

In Figure 6 we present the predictions for the A_{LRFB} asymmetry in several approximations, namely at the Born level and with 1-loop weak, pure QED, and complete EW contributions.

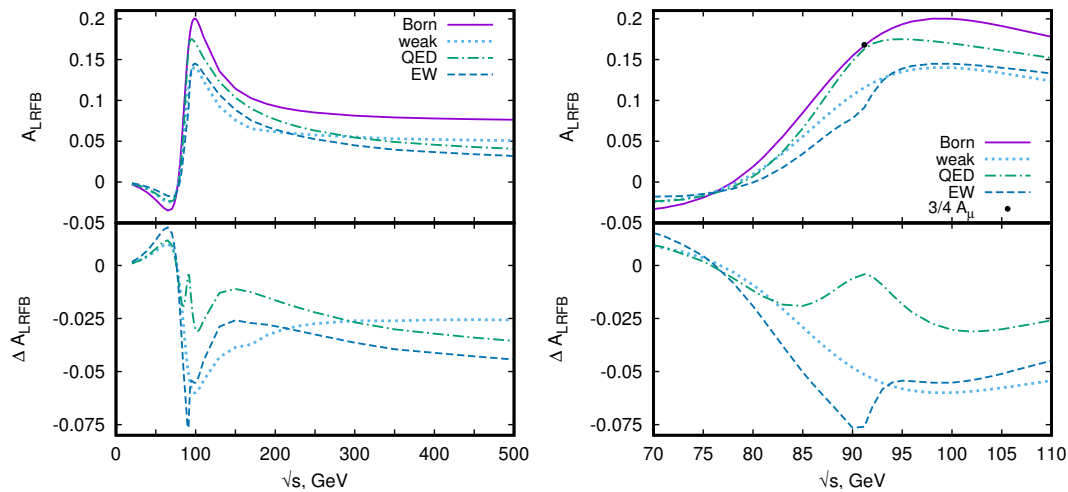


Figure 6. (Left) The A_{LRFB} asymmetry in the Born and 1-loop (weak, QED, EW) approximations and ΔA_{LRFB} for c.m.s. energy range; (Right) the same for the Z peak region.

Next, we repeat the study of the A_{LRFB} asymmetry behavior in different EW schemes. We have illustrated the energy dependence of the A_{LRFB} asymmetry in $\alpha(0)$, G_μ , and $\alpha(M_Z^2)$ schemes and the corresponding ΔA_{LRFB} in Figure 7. The impact of weak corrections on A_{LRFB} is large. For example, the Born-level value of A_{LRFB} at the Z peak is about 0.17, while accounting for the weak RCs contribution reduces the asymmetry value down to ~ 0.11 .

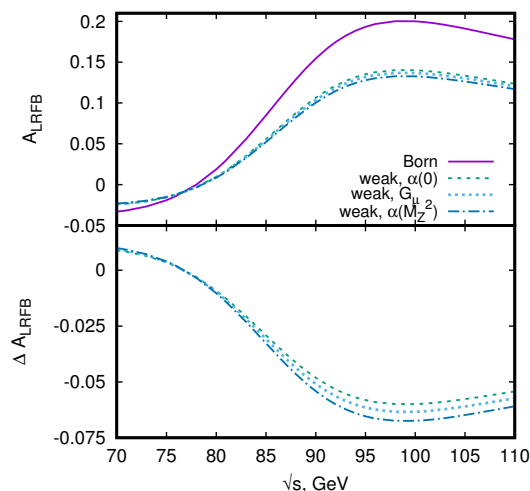


Figure 7. The A_{LRFB} asymmetry in the Born and 1-loop EW approximations and ΔA_{LRFB} within $\alpha(0)$, G_μ , and $\alpha(M_Z^2)$ EW schemes vs. c.m.s. energy in the Z peak region.

Summary for A_{LRFB}

We would like to emphasize that the above Formula (15) appears to be a rather rough approximation since radiative corrections shift the observable value of A_{LRFB} quite a lot. Apparently the A_{LRFB} asymmetry is more affected by weak corrections than A_{LR} . The shifts ΔA_{LRFB} only slightly depend on an EW scheme choice. The A_{LRFB} asymmetry at the Z boson peak depends on the final lepton coupling that could be used to measure the μ and τ weak couplings and their difference from the initial lepton (electron) one.

6. Final-State Fermion Polarization P_f

The polarization of a final-state fermion $P_{f=\mu,\tau}$ can be expressed as the ratio between the difference of the cross sections for right and left handed final state helicities and their sum

$$P_f = \frac{\sigma_{R_f} - \sigma_{L_f}}{\sigma_{R_f} + \sigma_{L_f}}. \quad (16)$$

In an experiment, it can be measured for the $\tau^+\tau^-$ channel by reconstructing the τ polarization from the pion spectrum in the decay $\tau \rightarrow \pi\nu$. Details of the analysis of P_τ measurements at LEP are described in [13]. Computer programs TAOLA [26] and KORALZ [27,28] were applied for this analysis. Estimated improvement for P_τ and τ decay products over LEP time in ILC in the GigaZ program was done in [5].

In the case for unpolarized beams in the vicinity of the Z peak, the expression for channel $e^+e^- \rightarrow \tau^+\tau^-$ is simplified to

$$P_\tau(\cos \vartheta_\tau) \approx - \frac{A_\tau + \frac{2 \cos \vartheta_\tau}{1 + \cos^2 \vartheta_\tau} A_e}{1 + \frac{2 \cos \vartheta_\tau}{1 + \cos^2 \vartheta_\tau} A_e A_\tau}. \quad (17)$$

From this observable, one can extract information on the couplings A_τ and A_e , simultaneously.

In Figure 8 (left) we show the distribution of P_τ in the cosine of the scattering angle at the Z peak in the Born and 1-loop (weak, QED, and EW) approximations. The same conventions as in previous sections are applied for the shifts ΔP_τ . The shift due to pure QED RCs is approximately a constant close to zero. But one can see that this observable is very sensitive to the presence of weak-interaction corrections.

In the presence of initial beams polarization the expression depends on P_{eff} :

$$P_\tau(\cos \vartheta) \approx - \frac{A_\tau(1 - A_e P_{\text{eff}}) + \frac{2 \cos \vartheta_\tau}{(1 + \cos^2 \vartheta_\tau)} (A_e - P_{\text{eff}})}{(1 - A_e P_{\text{eff}}) + \frac{2 \cos \vartheta_\tau}{(1 + \cos^2 \vartheta_\tau)} A_\tau (A_e - P_{\text{eff}})}. \quad (18)$$

which can be reduced to the short form neglecting the $A_e A_\tau$ and $A_e P_{\text{eff}}$ terms:

$$P_\tau(\cos \vartheta_\tau) \approx -A_\tau - \frac{2 \cos \vartheta_\tau}{(1 + \cos^2 \vartheta_\tau)} (A_e - P_{\text{eff}}). \quad (19)$$

The influence of the initial particle polarization on P_τ at the Z peak is demonstrated in the Figure 8 (right). For comparison the unpolarized and two polarized cases (13) as functions of $\cos \vartheta_\tau$ are shown. It is seen that the behavior of P_τ depends on the polarization set choices very much, note that it even changes the sign for the P_2 case. The corresponding shifts ΔP_τ also strongly depend on the initial beam polarization degrees and change the shape accordingly (note the maximum for P_1).

In Figure 9 we show the dependence of P_τ on the c.m.s. energy in the Born and 1-loop approximations (weak, QED, and EW). We see that at energies above the Z resonance, both weak and QED radiative corrections to P_τ are large and considerable cancellations happen between their contributions. Note that theoretical uncertainties in weak and QED RCs are not correlated, so it is necessary to take into account higher-order effects to reduce the resulting uncertainty in the complete 1-loop result for P_τ at high energies.

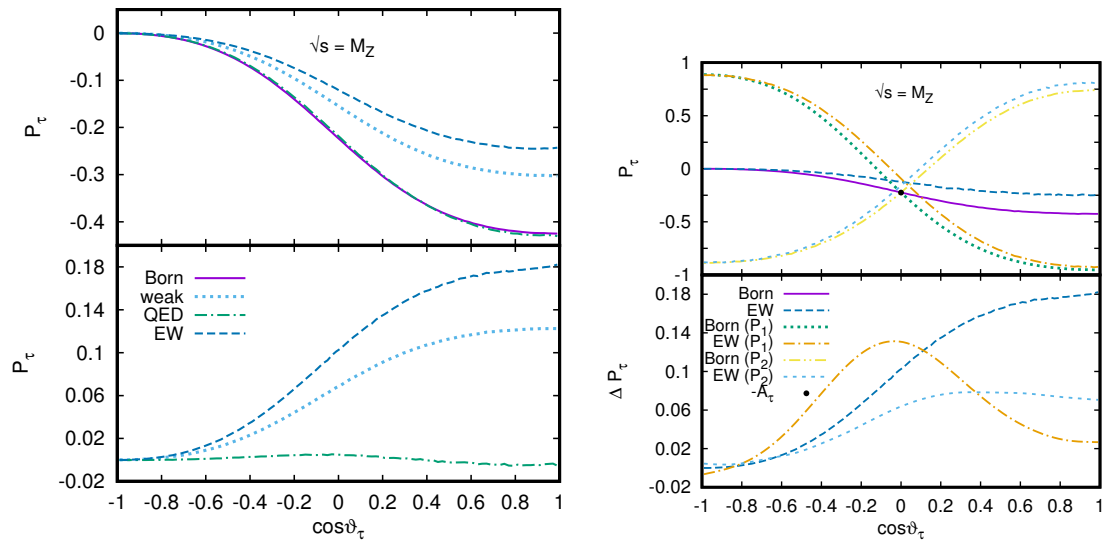


Figure 8. (Left) The P_τ polarization in the Born and 1-loop (weak, pure QED, and EW) approximations as a function of $\cos \theta_\tau$ at $\sqrt{s} = M_Z$. (Right) The P_τ polarization for unpolarized and polarized cases with (13) degrees of initial beam polarizations in the Born and EW 1-loop approximations vs. cosine of the final τ lepton scattering angle at the Z peak.

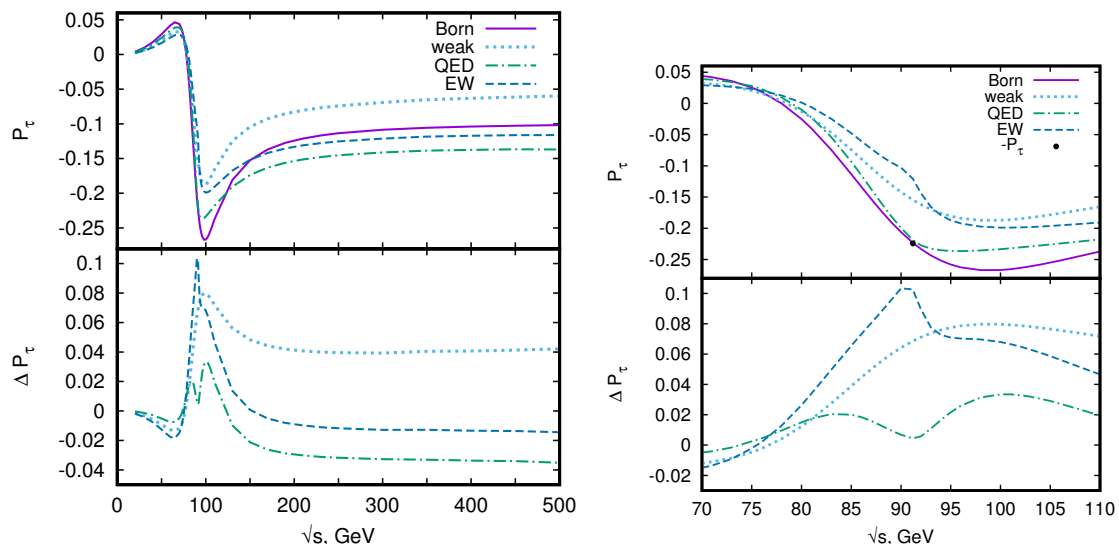


Figure 9. (Left) The P_τ polarization in the Born and 1-loop (weak, pure QED, and EW) approximations and ΔP_τ vs. c.m.s. energy in a wide range; (Right) the same for the Z peak region. The black dot indicates the value P_τ at the Z resonance.

In Figure 10 we show P_τ in the Born and 1-loop EW approximations for different sets of beam polarization degrees in a narrow bin around the Z resonance. The beam polarizations sets P_1 and P_2 are defined in Equation (13). One can see that the energy dependence of P_τ is strongly affected by a beam polarization choice outside the Z peak region. The same concerns the size of radiative corrections to P_τ , which are represented on the lower plot.

Summary for P_τ

The P_τ asymmetry is very sensitive to weak-interaction corrections and to the polarization degrees of the initial beams. Near the Z resonance the value of theoretical uncertainty of P_τ is determined by the interplay of uncertainties of rather large contributions pure QED and weak radiative corrections.

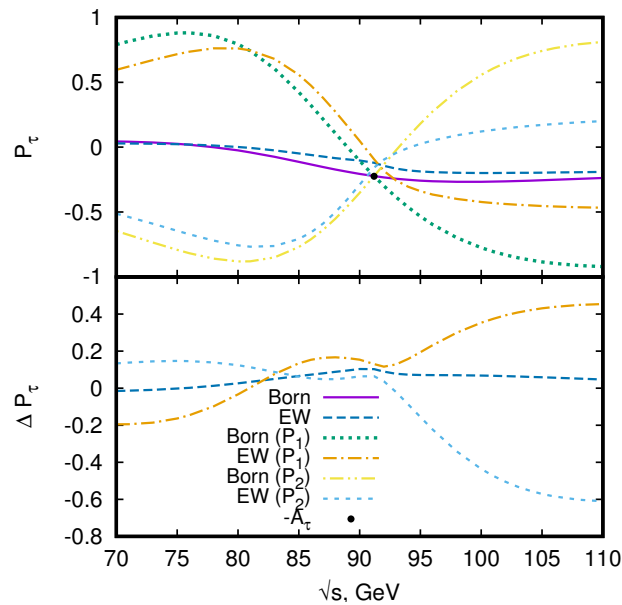


Figure 10. The P_τ polarization for (13) degrees of the initial beam polarizations in the Born and 1-loop EW approximations vs. c.m.s. energy in the Z peak region.

7. Conclusions

New opportunities of the future e^+e^- colliders: GigaZ options and new energy scale up to several TeV require modern tools for high-precision theoretical calculations of observables. We investigated A_{LR} , A_{FB} and A_{LRFB} for $e^+e^- \rightarrow \mu^+\mu^-$ channel and polarization P_τ for the final state in $e^+e^- \rightarrow \tau^+\tau^-$ channel on the Z resonance and in the high energy region up to 500 GeV by using MCSANC. We evaluated the resulting shifts of asymmetries at the Born and EW levels of accuracy in different EW schemes. The numerical results presented above for pure QED, weak, and complete EW radiative corrections show an interplay between the weak and QED contributions to asymmetries. This fact indicates the necessity to consider those contributions always in combined way.

Asymmetries in e^+e^- annihilation processes provide a powerful tool for investigation of symmetries between three fermion generations. By studying all available asymmetries, one can extract parameters of weak interactions in the neutral current for all three charged leptons. So, by comparing the parameters it will be possible to verify the lepton universality hypothesis at a new level of precision.

Hypothetical extra neutral Z' vector bosons [29] can contribute to the processes of e^+e^- annihilation. For example, effects of Kaluza–Klein excited vector bosons in the gauge Higgs unification on e^+e^- annihilation cross sections were considered in [30,31]. Since the new bosons can have couplings to left and right fermions being different from the SM ones, the asymmetries (especially with polarized beams) can help a lot in search for such Z' bosons.

At the FCC-ee we have experimental precision tag in the $\sin^2 \theta_W^{\text{eff}}$ measurement of the order of 5×10^{-6} , which means more than a thirty-fold improvement with respect to the current precision of 1.6×10^{-4} . This is due to a factor of several hundred improvement on statistical errors and because of a considerable improvement in particle identification and vertexing. In order to provide theoretical predictions for the considered asymmetries with sufficiently small uncertainties which would not spoil the precision of the future experiments besides the complete 1-loop EW radiative corrections presented here we need:

- higher order pure QED corrections preferably with resummation;
- higher order (electro)weak corrections;
- taking into account perturbative and nonperturbative quantum chromodynamics (QCD) effects in RCs;
- Monte Carlo event generators and integrators which ensure the required technical precision.

Challenges in calculations of higher order QED effects for FCC-ee were discussed in Ref. [32]. The complete two-loop electroweak corrections in the vicinity of the Z boson peak have been presented in [33]. More details on challenges for high-precision theoretical calculations for future e^+e^- colliders can be found in [34,35].

Author Contributions: Conceptualization, A.A., S.B. and L.K.; methodology, A.A., S.B. and L.K.; software, A.A., S.B. and L.K.; validation, A.A., S.B. and L.K.; formal analysis, A.A., S.B. and L.K.; investigation, A.A., S.B. and L.K.; resources, A.A., S.B. and L.K.; data curation, A.A., S.B. and L.K.; writing—original draft preparation, A.A., S.B. and L.K.; writing—review and editing, A.A., S.B. and L.K. The authors claim to have contributed equally and significantly in this paper. All authors have read and agreed to the published version of the manuscript.

Funding: This research was funded by RFBR grant 20-02-00441.

Acknowledgments: The authors are grateful to Ya. Dydyshka, R. Sadykov, V. Yermolchuk, and A. Saponov for fruitful discussions and numerical cross checks, and to A. Kalinovskaya for the help with preparation of the manuscript.

Conflicts of Interest: The authors declare no conflict of interest.

Abbreviations

The following abbreviations are used in this manuscript:

| | |
|--------|-------------------------|
| SM | Standard Model |
| QED | quantum electrodynamics |
| QCD | quantum chromodynamics |
| EW | electroweak |
| RCs | radiative corrections |
| FB | forward–backward |
| LR | left–right |
| c.m.s. | center-of-mass system |

References

1. Fujii, K.; Grojean, C.; Peskin, M.E.; Barklow, T.; Gao, Y.; Kanemura, S.; Kim, H.; List, J.; Nojiri, M.; Perelstein, M.; et al. Tests of the Standard Model at the International Linear Collider. *arXiv* **2019**, arXiv:1908.11299.
2. *A Multi-TeV Linear Collider Based on CLIC Technology: CLIC Conceptual Design Report*; SLAC National Accelerator Lab.: Menlo Park, CA, USA, 2012. [CrossRef]
3. Moortgat-Pick, G. The Role of polarized positrons and electrons in revealing fundamental interactions at the linear collider. *Phys. Rep.* **2008**, *460*, 131–243. [CrossRef]
4. The International Linear Collider Technical Design Report—Volume 2: Physics. *arXiv* **2013**, arXiv:1306.6352.
5. Bambade, P.; Barklow, T.; Behnke, T.; Berggren, M.; Brau, J.; Burrows, P.; Denisov, D.; Faus-Golfe, A.; Foster, B.; Fujii, K.; et al. The International Linear Collider: A Global Project. *arXiv* **2019**, arXiv:1903.01629.
6. Abada, A. FCC-ee: The Lepton Collider: Future Circular Collider Conceptual Design Report Volume 2. *Eur. Phys. J. ST* **2019**, *228*, 261–623. [CrossRef]
7. Ahmad, M.; Alves, D.; An, H.; An, Q.; Arhrib, A.; Arkani-Hamed, N.; Ahmed, I.; Bai, Y.; Ferroli, R.B.; Ban, Y.; et al. CEPC-SPPC Preliminary Conceptual Design Report. 1. Physics and Detector. Preprint IHEP-CEPC-DR-2015-01. 2015. Available online: <https://inspirehep.net/literature/1395734> (accessed on 1 June 2020).
8. Bhupal Dev, P.; Djouadi, A.; Godbole, R.; Muhlleitner, M.; Rindani, S. Determining the CP properties of the Higgs boson. *Phys. Rev. Lett.* **2008**, *100*, 051801. [CrossRef]
9. Hagiwara, K.; Ma, K.; Yokoya, H. Probing CP violation in e^+e^- production of the Higgs boson and toponia. *JHEP* **2016**, *6*, 48. [CrossRef]

10. Ma, K. Enhancing CP Measurement of the Yukawa Interactions of Top-Quark at e^-e^+ Collider. *Phys. Lett. B* **2019**, *797*, 134928. [\[CrossRef\]](#)
11. Erler, J.; Heinemeyer, S.; Hollik, W.; Weiglein, G.; Zerwas, P. Physics impact of GigaZ. *Phys. Lett. B* **2000**, *486*, 1389–1402. [\[CrossRef\]](#)
12. Grunewald, M. Experimental tests of the electroweak standard model at high-energies. *Phys. Rep.* **1999**, *322*, 125–346. [\[CrossRef\]](#)
13. Schael, S. Precision electroweak measurements on the Z resonance. *Phys. Rep.* **2006**, *427*, 257–454. [\[CrossRef\]](#)
14. Mnich, J. Experimental tests of the standard model in $e^+e^- \rightarrow f \text{ anti-}f$ at the Z resonance. *Phys. Rep.* **1996**, *271*, 181–266. [\[CrossRef\]](#)
15. Arbuzov, A.; Awramik, M.; Czakon, M.; Freitas, A.; Grunewald, M.; Monig, K.; Riemann, S.; Riemann, T. ZFITTER: A Semi-analytical program for fermion pair production in e^+e^- annihilation, from version 6.21 to version 6.42. *Comput. Phys. Commun.* **2006**, *174*, 728–758. [\[CrossRef\]](#)
16. Montagna, G.; Nicosini, O.; Piccinini, F.; Passarino, G. TOPAZ0 4.0: A New version of a computer program for evaluation of deconvoluted and realistic observables at LEP-1 and LEP-2. *Comput. Phys. Commun.* **1999**, *117*, 278–289. [\[CrossRef\]](#)
17. Bondarenko, S.; Dydyshka, Y.; Kalinovskaya, L.; Sadykov, R.; Yermolchik, V. One-loop electroweak radiative corrections to lepton pair production in polarized electron-positron collisions. *arXiv* **2020**, arXiv:2005.04748.
18. Andonov, A.; Arbuzov, A.; Bardin, D.; Bondarenko, S.; Christova, P.; Kalinovskaya, L.; Nanava, G.; von Schlippe, W. SANCscope—v.1.00. *Comput. Phys. Commun.* **2006**, *174*, 481–517. [\[CrossRef\]](#)
19. Arbuzov, A.; Bondarenko, S.; Dydyshka, Y.; Kalinovskaya, L.; Rumyantsev, L.; Sadykov, R.; Yermolchik, V. Electron-positron annihilation processes in MCSANee. *CERN Yellow Rep. Monogr.* **2020**, *3*, 213–216. [\[CrossRef\]](#)
20. Arbuzov, A.; Bardin, D.; Bondarenko, S.; Christova, P.; Kalinovskaya, L.; Klein, U.; Kolesnikov, V.; Rumyantsev, L.; Sadykov, R.; Saponov, A. Update of the MCSANC Monte Carlo integrator, v. 1.20. *JETP Lett.* **2016**, *103*, 131–136. [\[CrossRef\]](#)
21. Blondel, A. A Scheme to Measure the Polarization Asymmetry at the Z Pole in LEP. *Phys. Lett. B* **1988**, *202*, 145. [\[CrossRef\]](#)
22. Janot, P. Direct measurement of $\alpha_{QED}(m_Z^2)$ at the FCC-ee. *JHEP* **2016**, *2*, 53. [\[CrossRef\]](#)
23. Jadach, S.; Yost, S. QED Interference in Charge Asymmetry Near the Z Resonance at Future Electron-Positron Colliders. *Phys. Rev. D* **2019**, *100*, 013002. [\[CrossRef\]](#)
24. Arbuzov, A.; Bardin, D.; Leike, A. Analytic final state corrections with cut for $e^+e^- \rightarrow$ massive fermions. *Mod. Phys. Lett. A* **1992**, *7*, 2029–2038. [\[CrossRef\]](#)
25. Blondel, A.; Lynn, B.; Renard, F.; Verzegnassi, C. Precision Measurements of Final State Weak Coupling from Polarized Electron—Positron Annihilation. *Nucl. Phys. B* **1988**, *304*, 438–450. [\[CrossRef\]](#)
26. Jadach, S.; Was, Z.; Decker, R.; Kuhn, J.H. The tau decay library TAUOLA: Version 2.4. *Comput. Phys. Commun.* **1993**, *76*, 361–380. [\[CrossRef\]](#)
27. Jadach, S.; Ward, B.; Was, Z. The Monte Carlo program KORALZ, version 4.0, for the lepton or quark pair production at LEP/SLC energies. *Comput. Phys. Commun.* **1994**, *79*, 503–522. [\[CrossRef\]](#)
28. Jadach, S.; Ward, B.; Was, Z. The Monte Carlo program KORALZ, for the lepton or quark pair production at LEP/SLC energies: From version 4.0 to version 4.04. *Comput. Phys. Commun.* **2000**, *124*, 233–237. [\[CrossRef\]](#)
29. Langacker, P. The Physics of Heavy Z' Gauge Bosons. *Rev. Mod. Phys.* **2009**, *81*, 1199–1228. [\[CrossRef\]](#)
30. Funatsu, S.; Hatanaka, H.; Hosotani, Y.; Orikasa, Y. Distinct signals of the gauge-Higgs unification in e^+e^- collider experiments. *Phys. Lett. B* **2017**, *775*, 297–302. [\[CrossRef\]](#)
31. Funatsu, S. Forward-backward asymmetry in the gauge-Higgs unification at the International Linear Collider. *Eur. Phys. J. C* **2019**, *79*, 854. [\[CrossRef\]](#)
32. Jadach, S.; Skrzypek, M. QED challenges at FCC-ee precision measurements. *Eur. Phys. J. C* **2019**, *79*, 756. [\[CrossRef\]](#)
33. Dubovyk, I.; Freitas, A.; Gluza, J.; Riemann, T.; Usovitsch, J. Electroweak pseudo-observables and Z-boson form factors at two-loop accuracy. *JHEP* **2019**, *8*, 113. [\[CrossRef\]](#)

34. Blondel, A.; Freitas, A.; Gluza, J.; Riemann, T.; Heinemeyer, S.; Jadach, S.; Janot, P. Theory Requirements and Possibilities for the FCC-ee and other Future High Energy and Precision Frontier Lepton Colliders. *arXiv* **2019**, arXiv:1901.02648.
35. Blondel, A.; Gluza, J.; Jadach, S.; Janot, P.; Riemann, T. (Eds.) *Theory for the FCC-ee: Report on the 11th FCC-ee Workshop Theory and Experiments*; Vol. 3/2020; CERN Yellow Reports: Monographs; CERN: Geneva, Switzerland, 2019. [[CrossRef](#)]



© 2020 by the authors. Licensee MDPI, Basel, Switzerland. This article is an open access article distributed under the terms and conditions of the Creative Commons Attribution (CC BY) license (<http://creativecommons.org/licenses/by/4.0/>).